Subsurface sites of Fe in H/Si(111) studied by scanning tunneling microscopy

Markus Gruyters, Torben Pingel, and Richard Berndt
Institut für Experimentelle und Angewandte Physik, Christian-Albrechts-Universität zu Kiel, D-24098 Kiel, Germany
(Received 1 November 2012; revised manuscript received 21 March 2013; published 3 April 2013)

The structural and electronic properties of Fe atoms in the subsurface region of hydrogen-passivated Si(111) surfaces are investigated by scanning tunneling microscopy (STM). In the STM images, Fe atoms show a characteristic triangular structure with orientation and dimensions that match the Si host lattice. Comparison between atomically resolved microscopy images and the crystalline structure of the H/Si(111) surface indicate that Fe atoms occupy substitutional sites which are located in the third Si layer underneath the surface.

DOI: 10.1103/PhysRevB.87.165405 PACS number(s): 68.37.Ef, 68.47.Fg, 68.35.Dv

I. INTRODUCTION

In spintronics, the electron spin is used as an additional degree of freedom to develop a new generation of electronic devices.[1,2] A fundamental requirement is the existence of spin-polarized carriers. The latter are most naturally provided by ferromagnetic 3*d* transition metals and their alloys and compounds. Metals are therefore the basic components in current technological applications such as giant magnetoresistance devices.[1,2] Major advances in device development are possible by implementing spintronics in semiconductor technology. In common semiconductors, however, the existence of spin-polarized carriers is not an intrinsic property.

A primary goal of semiconductor spintronics is to establish appropriate sources of spin-polarized carriers. Two basic approaches exist. The first one relies on heterostructures, where spin-polarized carriers are injected into the semiconductor from a ferromagnet. The second one relies on diluted magnetic semiconductors, where spin-polarized carriers are induced by doping with transition-metal atoms. In the latter case, the main challenge is to provide materials with ferromagnetic ordering temperatures sufficiently above operating temperatures of electronic devices.

During the last two decades, a focus of research on transition-metal-doped semiconductors have been III-V compounds such as GaAs.[3] In recent years, interest has also evolved on group-IV semiconductors such as Si and Ge. Si-based spintronics appears to be particularly promising because Si technology is the most mature semiconductor technology. Considering fundamental research, the study of simple model systems with low doping concentration provides a good starting point. Electronic and magnetic properties of these materials depend on dopant properties such as concentration, lattice location, and spatial ordering.[4–8] Significant differences in magnetization and spin polarization may occur for dopants located either on interstitial or substitutional sites. Recent density functional theory (DFT) calculations for Fe doping of bulk Si have shown that the interstitial site is energetically favored over the substitutional site,[6,7] which is in agreement with conclusions from experimental investigations over more than 30 years.[9]

In the vicinity of the surface, the occupation of host sites by impurities may be different from the bulk. For the Si(111)7 × 7 surface, e.g., the occupation of substitutional sites in the third and fourth layers by Fe, has been suggested on the basis of x-ray photoelectron diffraction experiments.[10,11] The occupation of Si subsurface sites by Fe is of interest in order to elucidate the early growth stages of Fe silicides on Si(111).[12,13] Moreover, because Fe_3Si is ferromagnetic with a relatively high Curie temperature of 840 K, these systems are relevant to study the integration of magnetism into semiconductor technology.[14–16]

Here, we report on the structural and electronic properties of Fe atoms in the subsurface region of hydrogen-passivated Si(111). Atomically resolved scanning tunneling microscopy (STM) at low temperature suggests that substitutional sites (Fig. 1) are the location of the Fe atoms.

II. EXPERIMENTAL DETAILS

Experiments were performed in an ultrahigh vacuum apparatus providing a base pressure of about 6×10^{-11} mbar. A home-built STM was operated at a temperature of 12 K. All STM images were recorded in constant current mode with the sample voltage V applied between the Si substrate (n-type, P-doped, ≈10 Ω cm resistivity) and the tunneling tip. For spectroscopy of differential conductance, the feedback loop of the tip was disabled and the derivative of the current I with respect to V (dI/dV) measured by a lock-in amplifier. Electrochemically etched W tips were cleaned *in situ* by Ar ion sputtering and annealing. Iron phthalcyanine (FePc) molecules were evaporated from a crucible of an electron beam evaporation source onto the surface of a wet chemically prepared H/Si(111) substrate[18] held at room temperature. Our original motivation was to investigate the molecules themselves on a substrate that was expected to couple rather weakly to the molecular states. However, the experiments showed that intact FePc molecules were absent. Instead, FePc served as sources of single Fe atoms. Alternatively, elemental metallic Fe was evaporated with a low rate of 0.4 monolayers/min from a wire (99.998% purity) wrapped around a heated tungsten filament.

III. RESULTS AND DISCUSSION

For all STM images, the color scale is chosen such that the clean and defect-free H/Si(111) substrate appears mainly in dark to light blue. STM images of a clean H/Si(111) surface with atomic resolution are shown in Fig. 2 for mainly occupied ($V < 0$) and mainly unoccupied ($V > 0$) electronic states. For $V < 0$ [Fig. 2(a)], a hexagonal protrusion structure is observed[19] where the bright round protrusions can be attributed

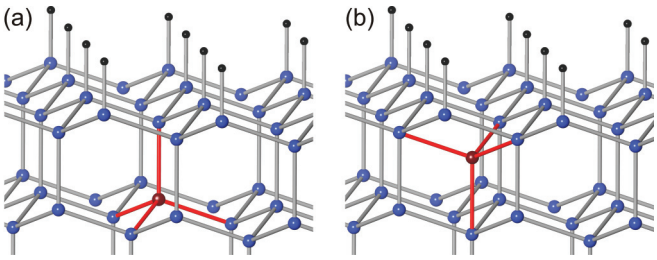

FIG. 1. (Color online) Schematic three-dimensional side view of the atomic structure of substitutional (a) and interstitial (b) sites in the diamond lattice of Si. Terminating H atoms are shown as small black spheres. Si atoms are shown as blue spheres. The first four Si layers of the H/Si(111) surface are shown. The image has been obtained using the program VESTA (Ref. 17).

to the location of H atoms on top of the first Si layer.[20] The lateral distance between neighboring protrusions is about 3.8 Å, which corresponds to the nearest-neighbor distance of Si atoms in an unreconstructed Si(111) surface.

For $V > 0$ [Fig. 2(b)], a honeycomblike structure with dark round depressions hexagonally arranged in a bright network[21] is observed at first sight. A closer inspection reveals that, additionally, there are hexagonally arranged protrusions superimposed on this network which also have lateral spacings of about 3.8 Å. It is assumed that for both $V > 0$ and $V < 0$, the brightest features correspond to the position of the H atoms on top of the first Si layer atoms, while the darkest features correspond to the position of the fourth Si layer atoms. This assignment is in line with density functional

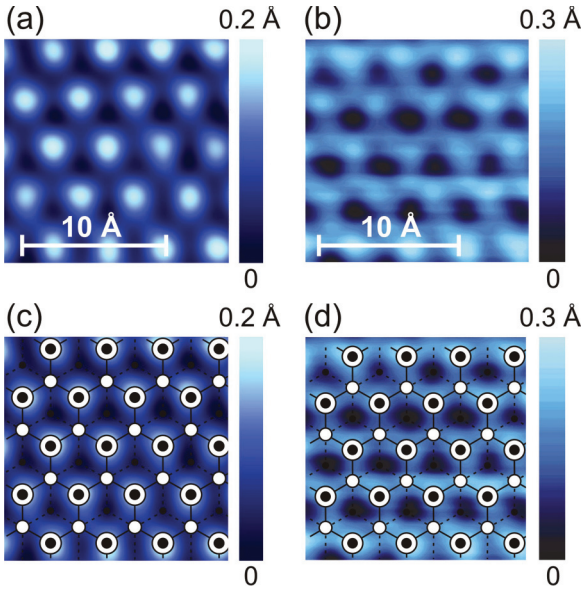

FIG. 2. (Color online) Constant current STM images of H/Si(111) with atomic resolution at different voltages [(a) $V = -2.2$ V, $I = 50$ pA and (b) $V = +2.0$ V, $I = 50$ pA]. (c) and (d) Same as (a) and (b), respectively, superimposed with schematic top view on the atomic structure of the H/Si(111) surface: First Si layer and H atoms: large white circles with central black circles; second Si layer atoms: white circles; fourth Si layer atoms: small black circles. First-to-second-layer bonds: solid black lines; third-to-fourth-layer bonds: dashed black lines.

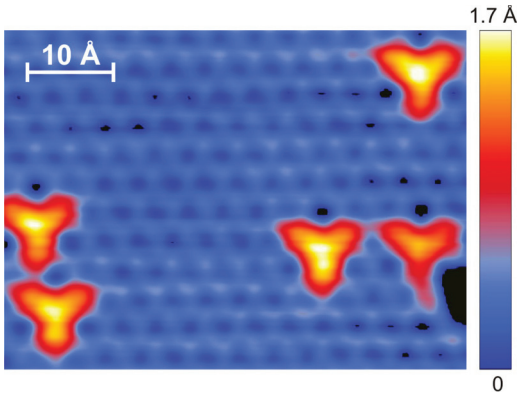

FIG. 3. (Color online) Constant current STM image of Fe-induced structures on H/Si(111) for a positive sample voltage ($V = +2.0$ V, $I = 50$ pA).

theory calculations of STM images for $V > 0$ (Ref. 22) and $V < 0$ (Ref. 20), respectively. The assignment of lattice sites is illustrated in Figs. 2(c) and 2(d), where a schematic top view on the atomic structure of the H/Si(111) surface is superimposed onto the STM images.

After evaporation of small amounts of FePc molecules onto the clean H/Si(111) surface, a characteristic triangular structure occurs in the STM images for positive sample voltages (Fig. 3). The spatial orientation of the triangular structure with respect to the H/Si(111) surface is always the same. It possesses maximum lateral dimensions of 10 Å and an apparent maximum height of 1.2 Å with respect to the H/Si(111) surface. For negative sample voltages, these structures change to depressions with radial symmetry (Fig. 4). The diameters of these holelike structures amount to ≈12 Å.

In the following, we discuss that the triangular and holelike structures originate from single Fe atoms underneath the surface. Before doing so, it should be noted that these structures can not be explained by intact FePc molecules. Single FePc molecules adsorbed on surfaces show the following common features in constant current STM images: first, lateral dimensions larger than 15 Å corresponding to the overall bond lengths of the molecule;[23–26] second, a fourfold symmetry corresponding to the four outer benzene rings[23–26] or, if the adsorption is nonplanar, signatures that correspond to the

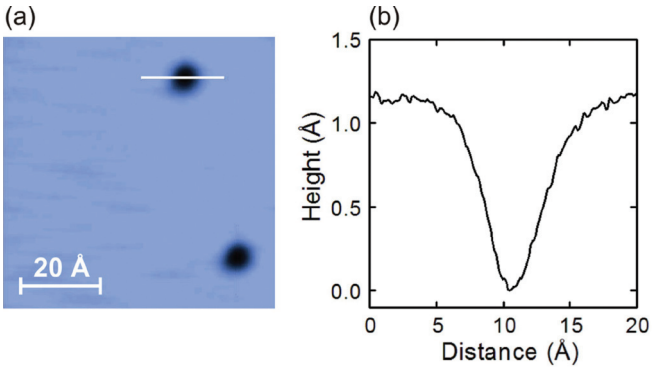

FIG. 4. (Color online) (a) Constant current STM image of Fe-induced structures on H/Si(111) for a negative sample voltage ($V = -2.5$ V, $I = 50$ pA). (b) Height profile along the white line in (a).

four outer benzene rings. Both these features, dimensions and shape, differ from the structures in Figs. 3 and 4 which leads to the assumption that FePc decomposes on the H/Si(111) surface. The molecule dissociates into its organic part and the central metal atom, the latter being responsible for the triangular and holelike structures in the STM images. Decomposition is found here for the H/Si(111) substrate held at room temperature during adsorption. If the substrate temperature is low, however, molecular adsorption takes place as evidenced by STM.[26]

It is well known that, for Fe metal deposition at room temperature, the first-deposited Fe atoms may react with the Si substrate, displacing Si atoms from their positions in the surface and subsurface layers.[12] Generally, the type of Fe location in Si depends on various parameters such as concentration, temperature, preparation method, and sample history. On the basis of x-ray photoelectron diffraction experiments, the occupation of substitutional sites in the third and fourth layers has been suggested for slight annealing of Fe deposited on Si(111)7×7 (Refs. 10 and 11) and H/Si(111) (Ref. 27) surfaces. Contrary to this, the occupation of interstitial sites by dissolved Fe is generally assumed for bulk Si at room temperature.[9]

In Figs. 5 and 6, a STM image of a typical single Fe-induced structure on H/Si(111) is analyzed in more detail. Height profiles (Fig. 6) along the white dashed arrows in Fig. 5(b) show a pronounced maximum at the center of the triangular structure, which may therefore rather be considered as a tripodlike structure. The height profiles show that the apparent height variations with a maximum of 1.2 Å induced by Fe are much larger than the height variations along the clean and unperturbed H/Si(111) surface which amount to only 0.3 Å. The H/Si(111) surface appears not to be only chemically but also to be electronically inert.

In the STM image, two additional Fe-induced features can be observed compared to the clean and unperturbed H/Si(111) surface: first, a relative decrease in apparent height of the three round dark blue depressions between the legs of the triangular structure [marked by "x" in Fig. 5(b)]; and second, a relative increase in apparent height of the round depressions at the ends of the legs of the triangular structure [indicated by "+" in Fig. 5(b)]. Fe-induced changes thus extend to a relatively large surface area [confined by the white triangle in Fig. 5(b)]. It should further be noted that all these changes match the atomic structure of the H/Si(111) host lattice.

In order to elucidate the exact location of the released Fe atom, the schematic top view on the atomic structure of H/Si(111) is superimposed on the STM image in Fig. 5(c). The clean and unperturbed H/Si(111) serves as a reference. The same assignment of lattice sites is used as discussed for Fig. 2, i.e., on H/Si(111), the brightest features correspond to the position of the first Si layer atoms, while the darkest features correspond to the position of the fourth Si layer atoms. According to this assignment, the maximum of the triangular structure corresponds to the position of a second Si layer atom [white circle in Fig. 5(c)]. Going from the center along the legs of the triangular structure, the next-neighboring atoms are on positions of fourth Si layer atoms [small black circles in Fig. 5(c)]. The most likely position of an Fe atom which corresponds to this ball-and-stick model consideration

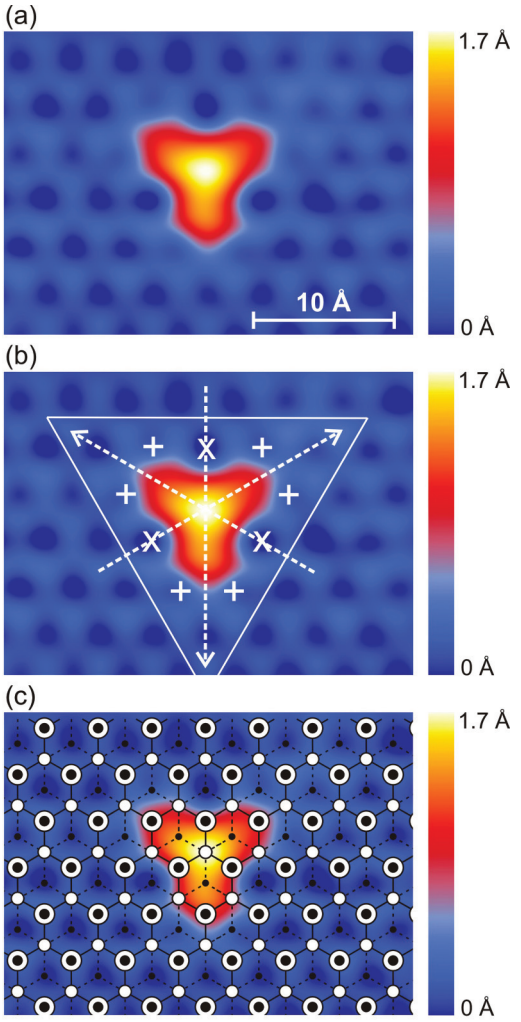

FIG. 5. (Color online) (a) Constant current STM image of a single Fe-induced structure on H/Si(111) with atomic resolution ($V = +2.0$ V, $I = 50$ pA), (b) superimposed with symbols and lines discussed in the text, (c) superimposed with schematic top view on the atomic structure of the H/Si(111) surface.

is a substitutional site in the third layer. In this case, the next-nearest neighbors of the Fe atom are three Si atoms in the fourth layer and one Si atom in the second layer directly

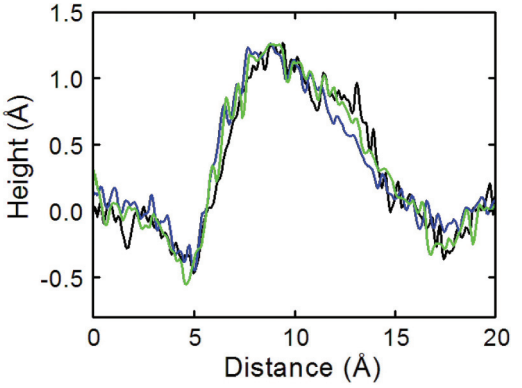

FIG. 6. (Color online) Height profiles along the white dashed arrows in Fig. 5(b). The maximum height on the clean and unperturbed H/Si(111) surface areas is set to zero.

on top of the third layer atom. This substitutional Fe site is schematically illustrated in Fig. 1(a).

For H/Si(111), a near-surface interstitial site would be located between second and third Si layer atoms, directly on top of a fourth Si layer atom [Fig. 1(b)]. This configuration can not be matched with the site assignment of Si atoms assumed in Fig. 2(d) for the following reason. If the maximum in apparent height of the triangular structure corresponded to the position of a fourth Si layer atom, then the deepest depressions on the H/Si(111) surface would correspond to the position of first or second Si layer atoms.

It is also unlikely that an Fe atom adsorbed on top of an intact H/Si(111) surface induces changes in the STM image which extend over distances larger than 20 Å as seen in Fig. 5. While STM images of single 3*d* transition-metal atoms on Si surfaces have not been reported, single Au atoms on Si(100) lead to circular structures with diameters of only 5 Å.[28] It can also be excluded that adsorption of single Fe atoms is accompanied by desorption of neighboring H atoms because Si-H bonds of hydrogen-passivated Si surfaces are strong and more stable than Si-Si bonds in the subsurface region.[29–31] For these two reasons and due to the tendency of transition-metal atoms to diffuse from the surface into Si,[12,32] on-surface adsorption appears to be unlikely.

Apart from these structural considerations, the question arises as to how the Fe-induced features in the STM image can be understood on the grounds of electronic properties of Fe impurities in Si. More precisely: How can the enhanced apparent height of the triangular structure and its characteristic shape be explained? Which electronic states are involved?

On the clean and unperturbed *n*-type H/Si(111) surface, electron tunneling should mainly occur into unoccupied states for $V = +2.0$ V (Ref. 33) even if tip-induced band bending[34] (TIBB) effects at the surface are taken into account. However, based on DFT calculations, light Fe doping of Si has been found to induce 3*d* electron-derived contributions in the electronic density of states (DOS) in the energy region around the Si band gap.[6,7] Hybridization takes place between t_{2g}-derived Fe 3*d* states with the neighboring Si sp^3 orbitals. Strong Fe-induced DOS changes occur in close vicinity to both the valence and conduction band edges of Si. For $V = +2.0$ V, TIBB (Ref. 33) may then lead to major electronic tunneling into states which are occupied under flat band condition. In other words, Fe 3*d*-induced occupied and/or unoccupied states near the Si band gap are likely to be the origin of the triangular structure observed in the STM images.

For $V < 0$, a holelike structure is obtained in the STM images (Fig. 4) which can not be attributed to electronic interaction of the Fe atom with neighboring Si atoms. Its origin should rather be explained by a local change of TIBB arising from the presence of the Fe atom. For *n*-type H/Si(111) at negative sample voltages, a tip-induced downward band bending leads to the formation of an accumulation region of electrons near the surface,[33] enabling electron tunneling from the substrate to the tip. However, electron tunneling may be inhibited if the downward bending is locally reduced due to electrostatic effects of the Fe atom. The magnitude of local change in TIBB depends on the lateral distance between the tip and the position of the Fe atom. With increasing distance, the influence of electrostatic effects of the Fe atom on TIBB decreases. In the STM image, a circular depression occurs around the position of the Fe atom which is not related to the electron density of states of the surface. A similar impurity-induced electronic effect on electron tunneling has been reported for STM images of P and B dopants in the subsurface region of Si(111)(2 × 1) (Ref. 35) and H/Si(100)(2 × 1),[36] respectively.

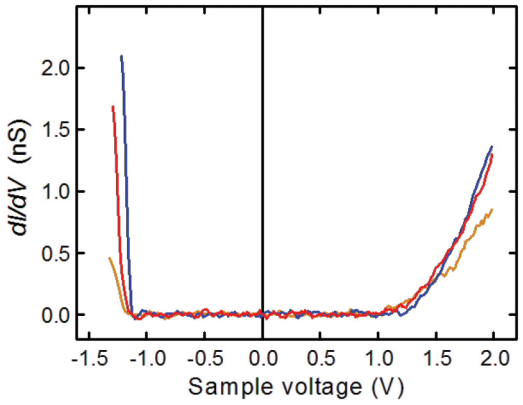

FIG. 7. (Color online) Spectra of dI/dV as a function of sample voltage at different positions: clean H/Si(111) surface (blue curve), end of leg (red curve), and center (orange) of the Fe-induced triangular structure. The spectra correspond to different tip-sample distances because in each case the feedback loop was opened at the same current and voltage (60 pA and +2.0 V).

Scanning tunneling spectroscopy (STS) could potentially be useful to obtain additional information on the Fe-induced feature. Spectra of dI/dV have therefore been recorded on the clean H/Si(111) surface and on different positions on the Fe-induced triangular structure (Fig. 7). On the clean H/Si(111) surface, dI/dV continuously increases with increasing (decreasing) sample voltage for $V > +1.0$ V ($V < -1.1$ V), reflecting the increase in local density of states with increasing (decreasing) energy distance from the conduction (valence) band edge. The dI/dV spectrum is similar to previous measurements on H/Si(111).[21] The lack of significant conductance in the voltage interval -1.1 V $< V < +1$ V reflects the semiconductor band gap. However, owing to a voltage drop in the semiconductor, the width of the conductance gap exceeds the band gap of Si (1.1 eV) as previously reported.[33] Neither peaks nor shoulders induced by Fe were observed in dI/dV spectra, merely a change in slope was found (Fig. 7).

Calculations of STM images for different subsurface and on-surface sites may be useful to confirm the suggested site of Fe. However, it should be mentioned that DFT, which has been used for the clean H/Si(111) surface, may not be most appropriate for treating transition-metal-induced features.[37] As in the case of transition-metal subsurface sites in GaAs(110), bulklike tight-binding approaches may have to be considered.[37–39]

It should also be mentioned that elemental metallic Fe has been deposited with a low rate of 0.4 monolayers/min onto H/Si(111) by evaporation from a heated wire. In the submonolayer regime, small Fe clusters of circular shape are formed with an average diameter of 20 Å and typical height from 2 to 6 Å. While we can not exclude the possibility that

single Fe atoms may be released to the Si subsurface region below these clusters, the data did not reveal any Fe-induced features in cluster-free areas of the surface.

IV. SUMMARY

A characteristic triangular structure has been found for Fe atoms at the H/Si(111) surface by atomically resolved scanning tunneling microscopy. Orientation and dimensions match the atomic structure of the Si substrate lattice. The structure is best explained by an Fe atom that occupies a substitutional site. This finding is particularly promising in view of DFT calculations including strong electron correlation effects[7] which result in a high-spin state connected with a half-metallic character for doping substitutional Fe into Si.

ACKNOWLEDGMENTS

We thank P. Kratzer and B. Geisler, Universität Duisburg-Essen, for discussions. Financial support by the Deutsche Forschungsgemeinschaft through Project No. GR 1409/5-1 is acknowledged.

[1] D. D. Awschalom and M. Flatté, Nat. Phys. **3**, 153 (2007), and references therein.
[2] M. Flatté, IEEE Trans. Electron Devices **54**, 907 (2007), and references therein.
[3] T. Jungwirth, J. Sinova, J. Mašek, J. Kučera, and A. H. MacDonald, Rev. Mod. Phys. **78**, 809 (2006), and references therein.
[4] P. R. Bandaru, J. Park, J. S. Lee, Y. J. Tang, L. H. Chen, S. Jin, S. A. Song, and J. R. O'Brien, Appl. Phys. Lett. **89**, 112502 (2006).
[5] H. Wu, P. Kratzer, and M. Scheffler, Phys. Rev. Lett. **98**, 117202 (2007).
[6] Z. Z. Zhang, B. Partoens, K. Chang, and F. M. Peeters, Phys. Rev. B **77**, 155201 (2008).
[7] F. Küwen, R. Leitsmann, and F. Bechstedt, Phys. Rev. B **80**, 045203 (2009).
[8] M. Shaughnessy, C. Y. Fong, R. Snow, L. H. Yang, X. S. Chen, and Z. M. Jiang, Phys. Rev. B **82**, 035202 (2010).
[9] A. A. Istratov, H. Hieslmair, and E. R. Weber, Appl. Phys. A **69**, 13 (1999), and references therein.
[10] A. Mascaraque, J. Avila, C. Teodorescu, M. C. Asensio, and E. G. Michel, Phys. Rev. B **55**, R7315 (1997), and references therein.
[11] E. G. Michel, Appl. Surf. Sci. **117**, 294 (1997).
[12] J. Alvarez, A. L. Vazquez de Parga, J. J. Hinarejos, J. de la Figuera, E. G. Michel, C. Ocal, and R. Miranda, Phys. Rev. B **47**, 16048 (1993).
[13] N. Onda, H. Sirringhaus, S. Goncalves-Conto, C. Schwarz, S. Zehnder, and H. von Känel, Appl. Surf. Sci. **73**, 124 (1993).
[14] S. Hong, P. Wetzel, G. Gewinner, D. Bolmont, and C. Pirri, J. Appl. Phys. **78**, 5404 (1995).
[15] J. Herfort, H. P. Schönherr, A. Kawaharazuka, M. Ramsteiner, and K. H. Ploog, J. Cryst. Growth **278**, 666 (2005).
[16] K. Ueda, R. Kizuka, H. Takeuchi, A. Kenjo, T. Sadoh, and M. Miyao, Thin Solid Films **515**, 8250 (2007).
[17] K. Momma and F. Izumi, J. Appl. Crystallogr. **44**, 1272 (2011).
[18] M. Gruyters, Surf. Sci. **515**, 53 (2002).
[19] K. Itaya, R. Sugawara, Y. Morita, and H. Tokumoto, Appl. Phys. Lett. **60**, 2534 (1992).
[20] Y. Li and G. Galli, Phys. Rev. B **82**, 045321 (2010).
[21] R. S. Becker, G. S. Higashi, Y. J. Chabal, and A. J. Becker, Phys. Rev. Lett. **65**, 1917 (1990).
[22] N. Lu, Ph.D. thesis, Iowa State University, 2010.
[23] H. J. Gao and L. Gao, Prog. Surf. Sci. **85**, 28 (2010), and references therein.
[24] L. Gao, W. Ji, Y. B. Hu, Z. H. Cheng, Z. T. Deng, Q. Liu, N. Jiang, X. Lin, W. Guo, S. X. Du, W. A. Hofer, X. C. Xie, and H. J. Gao, Phys. Rev. Lett. **99**, 106402 (2007).
[25] T. G. Gopakumar, T. Brumme, J. Kröger, C. Toher, G. Cuniberti, and R. Berndt, J. Phys. Chem. C **115**, 12173 (2011).
[26] M. Gruyters, T. Pingel, T. G. Gopakumar, N. Néel, Ch. Schütz, F. Köhler, R. Herges, and R. Berndt, J. Phys. Chem. C **116**, 20882 (2012).
[27] M. G. Martin, J. Avila, M. Gruyters, C. Teodorescu, P. Dumas, Y. J. Chabal, and M. C. Asensio, Appl. Surf. Sci. **123-124**, 156 (1998).
[28] F. Chiaravalloti, D. Riedel, G. Dujardin, H. P. Pinto, and A. S. Foster, Phys. Rev. B **79**, 245431 (2009).
[29] S. Jeong, Surf. Sci. **530**, 155 (2003).
[30] H. Jeong and S. Jeong, Phys. Rev. B **71**, 035310 (2005).
[31] D. R. Alfonso, C. Noguez, D. A. Drabold, and S. E. Ulloa, Phys. Rev. B **54**, 8028 (1996).
[32] A. Wawro, S. Suto, R. Czajka, and A. Kasuya, Phys. Rev. B **67**, 195401 (2003).
[33] M. McEllistrem, G. Haase, D. Chen, and R. J. Hamers, Phys. Rev. Lett. **70**, 2471 (1993).
[34] R. M. Feenstra, J. Vac. Sci. Technol. B **21**, 2080 (2003).
[35] T. Trappmann, C. Sürgers, and H. v. Löhneysen, Europhys. Lett. **38**, 177 (1997).
[36] M. Schöck, C. Sürgers, and H. v. Löhneysen, Phys. Rev. B **61**, 7622 (2000).
[37] J. K. Garleff, C. Çelebi, W. Van Roy, J. M. Tang, M. E. Flatté, and P. M. Koenraad, Phys. Rev. B **78**, 075313 (2008).
[38] D. Kitchen, A. Richardella, J. M. Tang, M. E. Flatté, and A. Yazdani, Nature (London) **442**, 436 (2006).
[39] J. M. Jancu, J. Ch. Girard, M. O. Nestoklon, A. Lemaître, F. Glas, Z. Z. Wang, and P. Voisin, Phys. Rev. Lett. **101**, 196801 (2008).